Supporting Online Material for

An ATP Gate Controls Tubulin Binding by the Tethered Head of Kinesin-1

Maria C. Alonso, Douglas R. Drummond, Susan Kain,
Julia Hoeng, Linda Amos, Robert A. Cross[1]*

*To whom correspondence should be addressed. E-mail: r.cross@mcri.ac.uk

Published 6 April 2007, *Science* **316**, 120 (2007)
DOI: 10.1126/science.1136985

This PDF file includes:

Materials and Methods
SOM Text
Figs. S1 to S4
References

Supplementary Material | Alonso et al | ATP-Gating mechanism of Kinesin

Supplementary Methods

1. Proteins & protein chemical methods

1.1 Proteins | Nkin460GST containing the N-terminal 460 amino acids of Neurospora kinesin-1 and a C-terminal GST fusion was prepared as described (*1*). Rat430GST protein (*2*) used in the steady state ATPase assays contained the equivalent 430 N-terminal amino acids of rat Kinesin-1 and a C-terminal GST fusion. This protein was a gift from Dr Isabelle Crevel. Rat rK430 as used in the FPLC gel filtration and the kinetics experiments was untagged. The insert for this construct was PCR amplified from a full length rat kinesin (kif5c clone) originally given to us by Scott Brady. Starting Oligo : 5'-CC GCT CTA CAT ATG GCG GAC CCA GCC GAA TGC AGC-3' Ending Oligo :5'-CCG ACT AGT CTA GAA TTC CTT GTC ATC CAG CTG-3'. The PCR product was digested with NdeI/SpeI and ligated into pET 17b. Expression and purification of the protein was according to (*3*). Pig brain tubulin was prepared according to Mitchison and Kirschner (*4*) (http://mitchison.med.harvard.edu/protocols.htm) and *S. pombe* tubulin by a modification of the method of Davis et al (*5*) to be described in detail elsewhere. Purified tubulins were desalted into PEM containing 20 μM GDP before storage in liquid nitrogen. Protein concentrations were determined by UV absorption scan of samples of protein dissolved in 6 M guanidine hydrochloride, correcting for background scattering by subtracting a scan of buffer alone, and assuming full nucleotide occupancy.

1.2 Steady state ATPase | The microtubule or tubulin heterodimer stimulated ATPase activity of kinesin was measured at 25°C using a pyruvate kinase / lactate dehydrogenase linked assay as described (*6*), except that microtubules were assembled in PEM (*7*) containing 1mM GMPCPP, pelleted and resuspended in PEM containing 10 nM GMPCPP before dilution into the linked assay buffer (20mM PIPES, pH 6.9, 5 mM $MgCl_2$, 1mM DTT, 0.1 mg ml^{-1} BSA). Tubulin heterodimers were diluted from a stock in PEM containing 20μM GDP. NAD/H absorption measurements were made in a Cary 50 spectrophotometer using disposable 50 μl UV transparent cuvettes (Eppendorf). Values for V_{max} and K_m were obtained by least squares fitting to plots of ATPase versus tubulin heterodimer concentration, using Kaleidagraph 3.6.4 (Synergy Software). ATPase values are per kinesin head.

1.3 Superose 12 gel filtration | Stock kinesin (typically 69 μM heads concentration in 20% glycerol, 20 mM phosphate buffer pH 7.0, 2 mM $MgCl_2$, 0.3 M NaCl, 0.1 mM DTT) was mixed with stock tubulin (typically 58 μM heterodimers in 50 mM PIPES pH 6.9, 0.2 mM $MgCl_2$, 1 mM EGTA, 0.1 μM Na-GTP, 30% glycerol) and adjusted to a final volume of 240μl and final concentrations of 6.5 μM kinesin heads and 13 μM tubulin heterodimers, with either no added nucleotide, or 2 mM AMPPNP or 2 mM ADP by adding 10x column buffer and water as necessary. The mixture was incubated for 10 mins on ice and centrifuged briefly in a microfuge (this was precautionary: no pellet was obtained). The entire 240 μl sample was then applied to a Superose HR 10/300 GL column held at 4°C and running at 0.5 ml min^{-1}. The column buffer was 50 mM PIPES pH 6.9, 2 mM $MgCl_2$, 1 mM EGTA; plus either nothing or 2 mM ADP or 0.2 mM AMPPNP. 0.3 ml fractions were collected. The reduced concentration of AMPPNP in the column buffer was found to be adequate and was used for reasons of cost. Elution patterns were monitored at 290 nm to avoid the large nucleotide contribution to the 280 nm absorbance. The kinesin absorbance is low because there are few tryptophans in the rK430 sequence. This is convenient because it means that the tubulin behaviour dominates the elution profiles from the mixtures.

1.4 Gel electrophoresis and densitometry | Samples from the peak fractions were run on
Invitrogen NuPAGE 10% bis-tris precast 15 well gels and run in MOPS (Invitrogen) buffer at 200 V for 1.5 hours. Gels were stained with SimplyBlue (Invitrogen) and imaged with a greyscale CCD camera. Quantitation was initially done using ImageJ (Rasband, W.S. (1997-2006); http://rsb.info.nih.gov/ij). Integrated optical density values for each band were corrected by subtracting the integrated optical density of a corresponding local area of featureless gel. The system was calibrated using an optical density wedge. In later work, we used the sypro organge fluorescent staining system (Molecular Probes, method exactly as per manufacturer's instructions) in combination with a Phosphorimager (Molecuar Dynamics) and BioRad Image Quant software. The two approaches gave comparable results. The numbers quoted in the text refer only to the Phosphorimager / Sypro red data.

1.5 Mant ATP turnover experiments | Stock tubulin (see above) was dialysed for 30 minutes against a large excess volume of 50mM PIPES pH 6.9, 0.2 mM $MgCl_2$, 1 mM EGTA, 10% glycerol to remove unbound guanidine nucleotides. The concentration of the
dialysed protein was determined by UV absorption scan (see above). Enzyme reactions were done in 20 mM PIPES pH 6.9, 2 mM $MgCl_2$, using quartz fluorimeter cuvettes. Fluorescence transients were recorded with a Cary Eclipse fluorimeter. At the start of the reaction, cuvettes contained 1 μM MantATP in 20 mM PIPES pH 6.9, 2 mM $MgCl_2$. To this we added kinesin to a final concentration of 1 μM kinesin heads, and in some experiments tubulin to a final concentration of 2 μM tubulin heterodimers. Then we "chased" by adding either 100 mM Na-ATP or 100 mM AMPPNP, to 1 mM final concentration. The final volume in every case was 600 μl. Experiments in which 4 μM of tubulin was added yielded essentially identical results (not shown).

2. Supplementary Data.

2.1 Superose 12 gel filtration of kinesin-tubulin mixtures

Figure S1 | Superose 12 chromatography of kinesin-tubulin mixtures
The data were obtained as described above and for Fig. 2 in the main text, and the axes are equivalent. The difference in this case is that a mixing ratio of 1 tubulin heterodimer per kinesin head was used. The tubulin peak (the rightmost peak visible in Fig. S1A and Fig. S1B) is then entirely shifted to an earlier elution position in Fig.S1C.

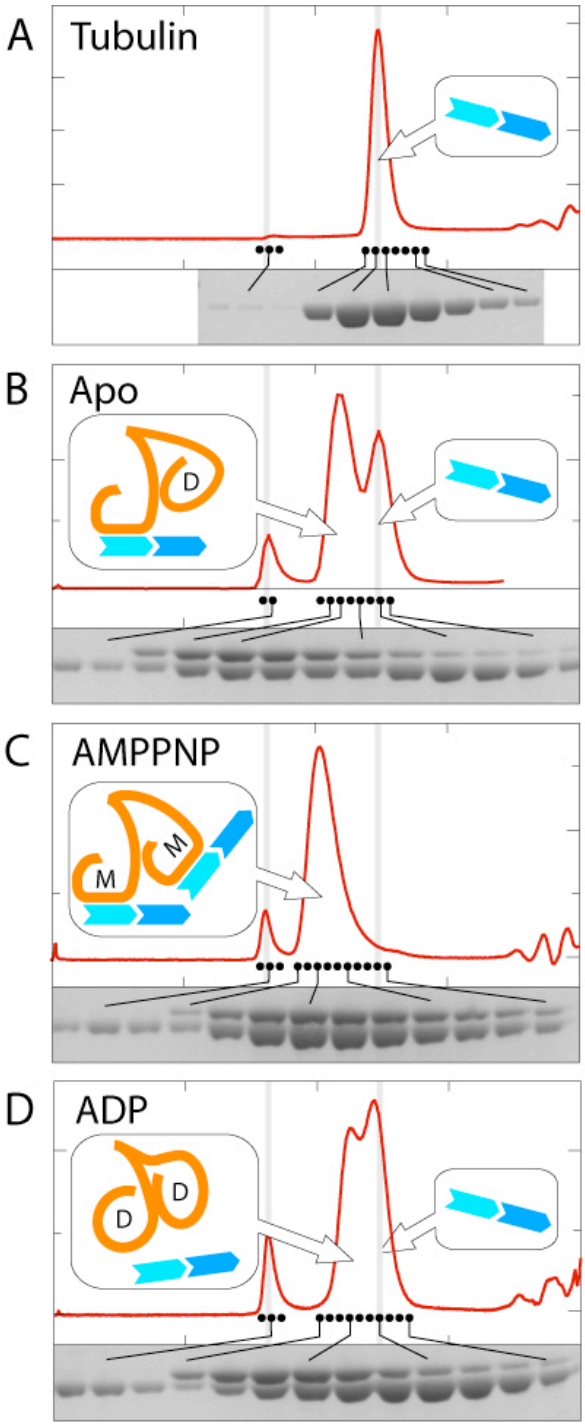

2.2 Docking tubulin heterodimers to the rat kinesin dimer (3KIN) crystal structure

Figure S2 (below) shows that the tubulin binding sites of 3KIN are positioned so that were tubulin heterodimers to bind to this structure, they would be spaced well apart and would not clash with one another. In 3KIN, both heads are occupied by ADP, and both neck linkers are docked. Our data show that only one tubulin heterodimer can bind to a kinesin dimer in the absence of AMPPNP. Fitting of cryoEM data suggests the possibility that the tubulin binding site in the second head is physically masked (below). Further work will be required to determine the structural mechanism by which the tubulin binding site on the second head is blocked.

Figure S2 | Docking tubulin heterodimers to the rat kinesin dimer (3KIN) crystal structure

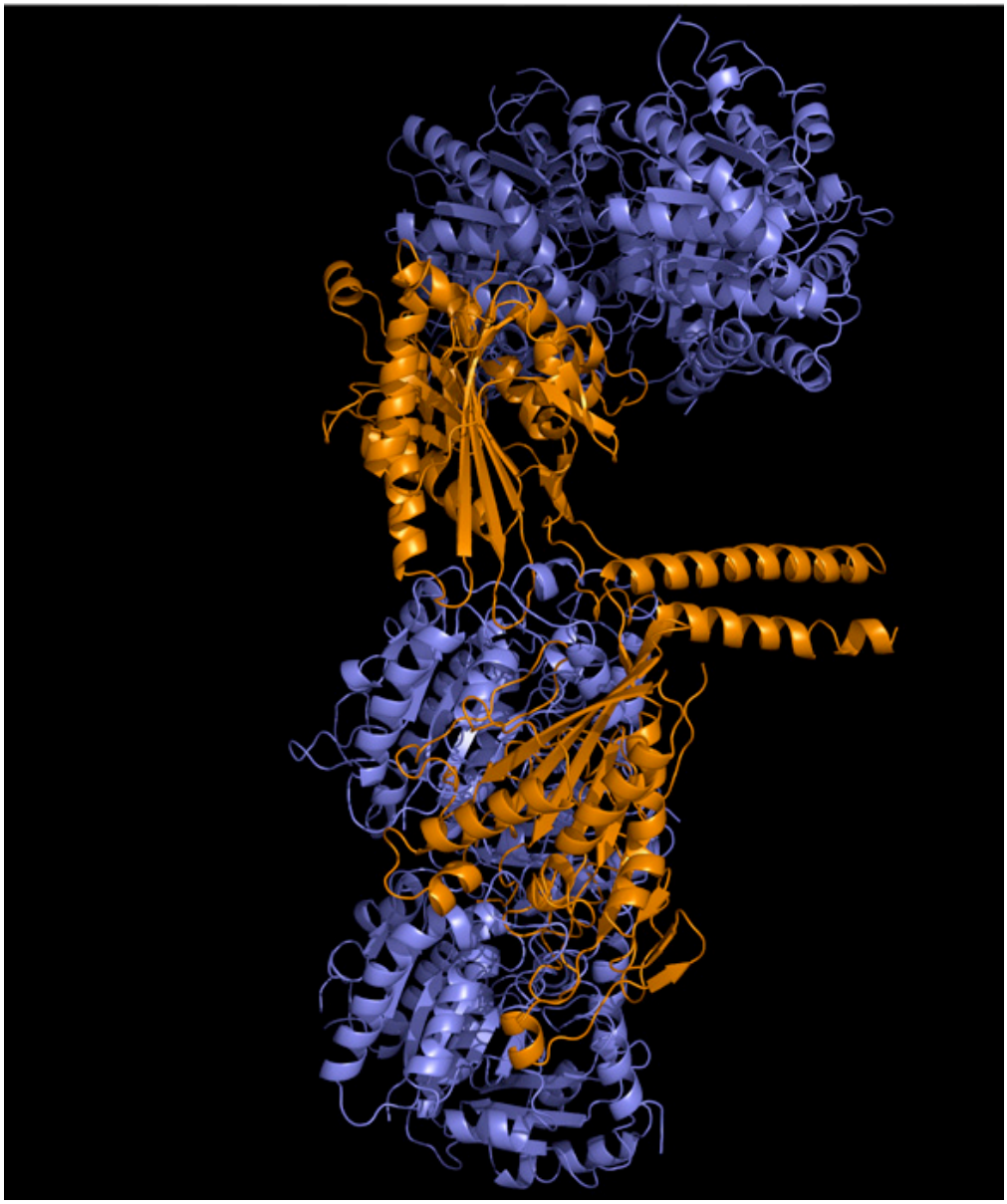

2.3 Docking a kinesin crystal structure into the parked head of a cryo-EM structure

The microtubule bound head

The cryo-EM surface contour map shown in **Fig. S3** is of 15-pf MTs decorated with dimeric rat kinesin-1 in the absence of free nucleotide (*8*), expected to correspond to the ATP-waiting dwell state in the walking mechanism. This map has a resolution of ~30Å.

Supplementary Figs. S4A-C show docking of a model comprising a tubulin protofilament with one kinesin head bound (white polypeptide backbone) into the CryoEM map (blue net). This model complex comprises tubulin and the motor domain of Kar3 in an orientation derived in separate experiments by docking into a high resolution cryo-EM map (*9*). The main contact with tubulin is made by helix α4 of the motor domain, as was also found for Kif1A (*10*). The crystal structures of kinesin-1's can be aligned to those of Kar3 with r.m.s. differences of 1.5-3 Å, so the tubulin-Kar3 complex serves as a sufficient model here.

The tethered head

We then considered the position of the second (tethered) head. Fitting was done by eye using one head of the rat kinesin dimer 3KIN, requiring that the two strands of the coiled coil neck of the dimer remain close. **Figs. S4A-C** show the tethered head in green. This approach yielded 2 possible dockings for the second head, A and B. Both these dockings for the second motor domain have the α-helical neck of the second motor domain in roughly the right region to pair into a coiled coil with that of the first motor domain.

Fig. S4A shows the front view of these two alternative fits. It is clear that docking A provides the better fit. Yellow arrows point to the stretch of helix that would form half of the coiled-coil stalk. The differences between the dockings are less distinct in other views (Fig.**S4B** & **S4C**) since the overall shape of the motor domain is roughly triangular, with up to 6 possible dockings.

Caveat

In doing this fitting, we considered the possibility that the bulk of the kinesin-1 motor domain may move relative to α4, as has been observed for Kif1A (*10, 11*), but not for Kar3 (*9*). If such a movement occurred, it would noticeably affect the position of the alpha helical coiled coil stalk but not the space available for docking the 2nd head. The work on Kar3 suggests that the top of the bound motor domain undergoes a significant conformational change in the apo state but there is no crystal structure for this state. Accordingly, the possibility that the main part of the head might shift relative to alpha 4 limits the precision of the fitting. Specifically, there is uncertainty about the precise position of the end of the neck linker of the the microtubule-bound head. Nonetheless the approximate fit obtained is robust, because the elongated shape of the head in combination with a requirement for close apposition of the two necks provides a sufficient constraint.

Conclusions

Higher resolution studies of tubulin and dimeric kinesin are required to establish the precise and unequivocal orientation for the second head. It is nonetheless clear that the most reasonable fit (docking A), leads to partial occlusion of the microtubule binding surface of the tethered head, suggesting that tubulin binding by the tethered head is inhibited in the dwell state by parking the tethered head against the bound head so as to mask its tubulin binding site.

Alonso et al Supplementary Fig.S3. CryoEM map of the dwell state (*8*)

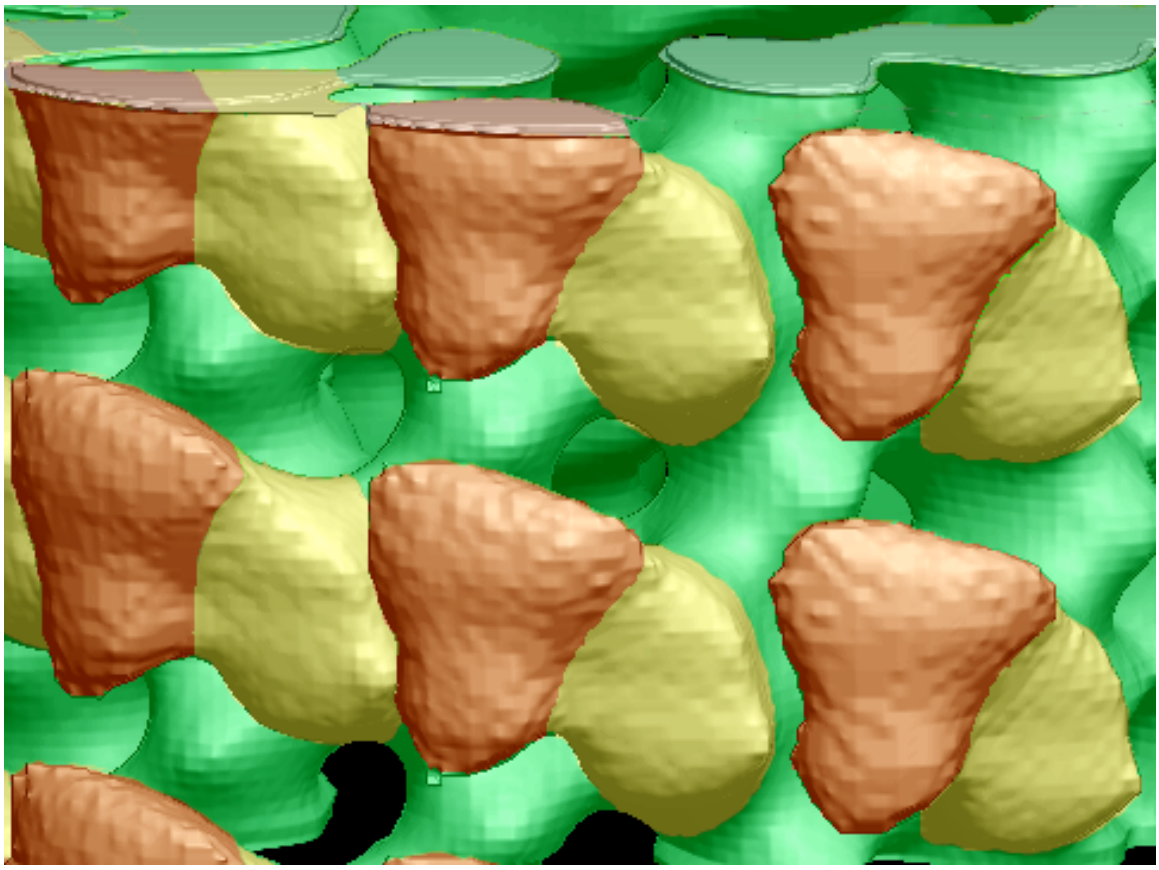

Alonso et al Supplementary Fig.S4. Fitting the cryoEM map.

Fig. S4A | Front View

Docking A Docking B

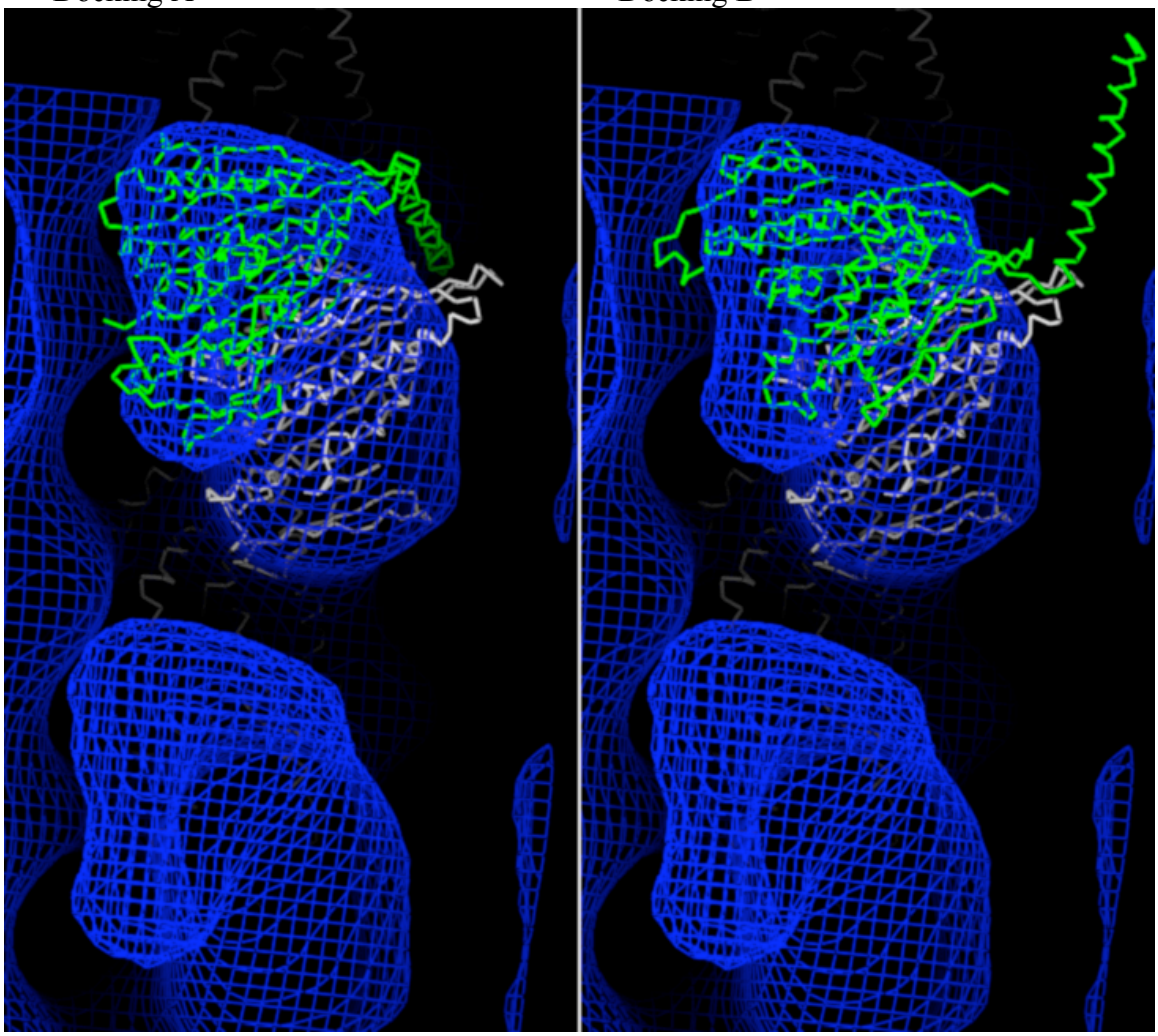

Fig. S4B | Side View

Docking A Docking B

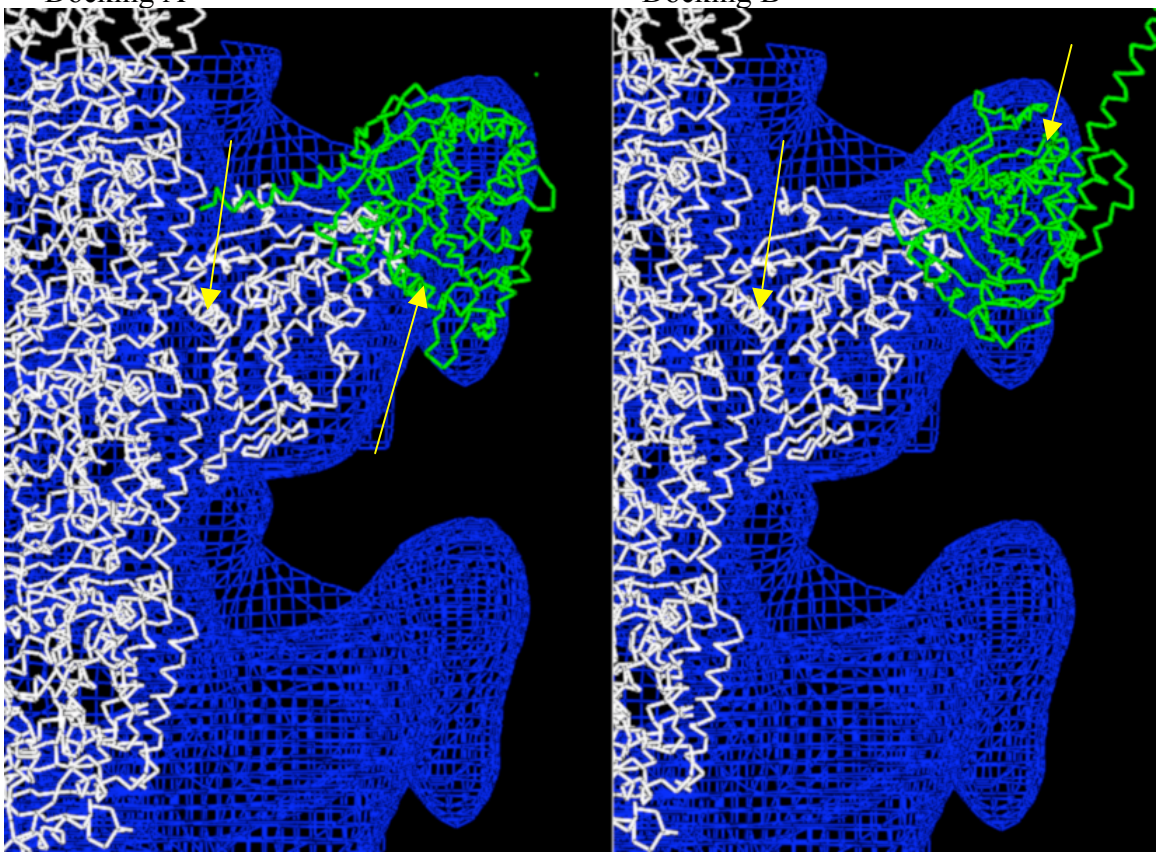

Fig. S4C |Top View

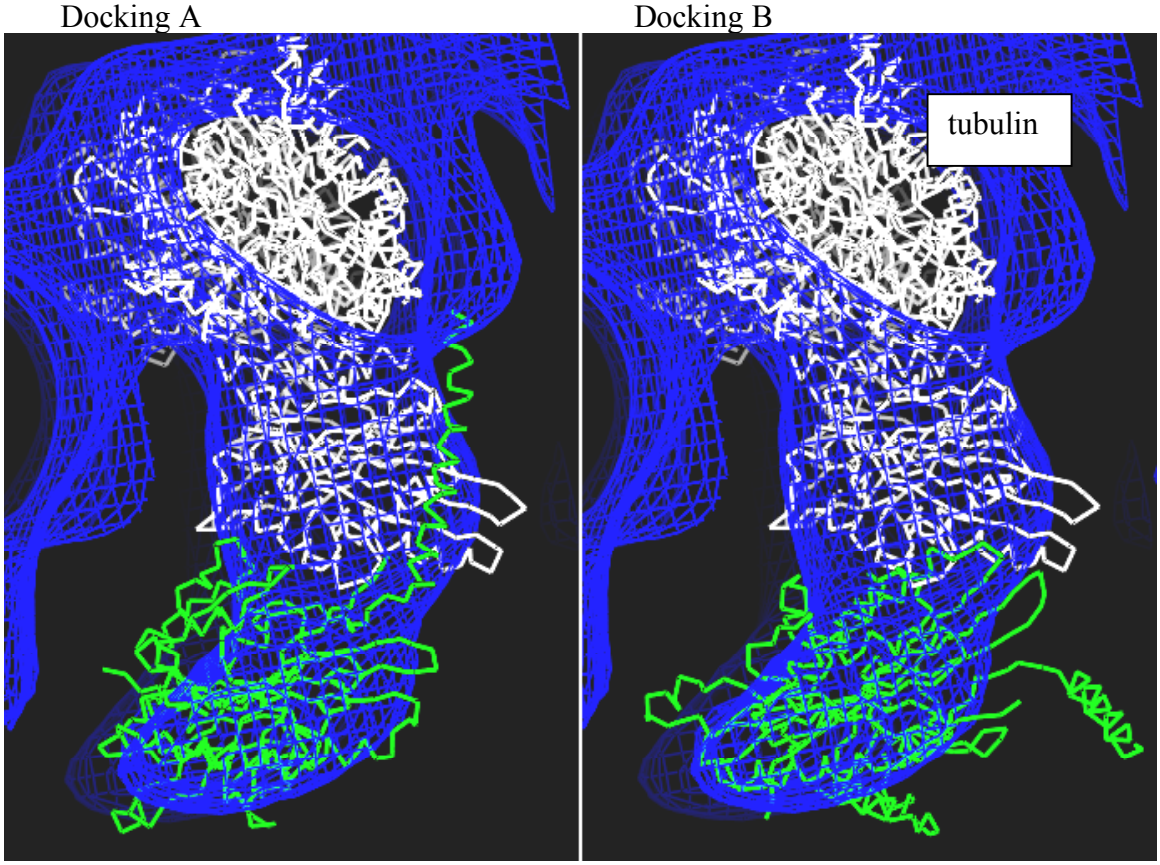

Supplementary References

1. I. Crevel, N. Carter, M. Schliwa, R. Cross, *Embo J* **18**, 5863 (1999).
2. I. M. Crevel, A. Lockhart, R. A. Cross, *J Mol Biol* **273**, 160 (1997).
3. A. Lockhart, I. M. Crevel, R. A. Cross, *J Mol Biol* **249**, 763 (1995).
4. T. Mitchison, M. Kirschner, *Nature* **312**, 232 (Nov 15-21, 1984).
5. A. Davis, C. R. Sage, L. Wilson, K. W. Farrell, *Biochemistry* **32**, 8823 (Aug 31, 1993).
6. A. Lockhart, R. A. Cross, *Embo J* **13**, 751 (1994).
7. J. W. Walker, G. P. Reid, J. A. McCray, D. R. Trentham, *J Am Chem Soc* **110**, 7170 (1988).
8. K. Hirose, J. Lowe, M. Alonso, R. A. Cross, L. A. Amos, *Mol Biol Cell* **10**, 2063 (1999).
9. K. Hirose, E. Akimaru, T. Akiba, S. A. Endow, L. A. Amos, *Mol Cell* **23**, 913 (Sep 15, 2006).
10. R. Nitta, M. Kikkawa, Y. Okada, N. Hirokawa, *Science* **305**, 678 (Jul 30, 2004).
11. M. Kikkawa, N. Hirokawa, *Embo J* (Aug 31, 2006).